ACS SENSORS

Article

Cite This: ACS Sens. XXXX, XXX, XXX−XXX

pubs.acs.org/acssensors

# Microencapsulated Immunoassays for Detection of Cytokines in Human Blood

Ali Rahimian,[†] Christian Siltanen,[‡] Hamid Feyzizarnagh,[†] Patricio Escalante,[§] and Alexander Revzin*,[†]

[†]Department of Physiology and Biomedical Engineering, Mayo Clinic, Rochester Campus, Rochester, Minnesota 55905, United States

[‡]Department of Bioengineering, University of California San Francisco, San Francisco, California 94158, United States

[§]Division of Pulmonary and Critical Care Medicine, Department of Medicine, and Mayo Clinic Center for Tuberculosis, Mayo Clinic, Rochester Campus, Rochester, Minnesota 55905, United States

Supporting Information

**ABSTRACT:** Cytokines are produced by leukocytes in blood and may be used as indicators of malignancies or infections. The objective of this study was to develop a strategy for immunosensing cytokines in whole, unprocessed human blood. Microfluidic droplet generation was employed to fabricate ∼400 μm diameter microcapsules with a hydrogel shell and an aqueous core containing sensing microbeads. The hydrogel shell was composed of poly(ethylene glycol) forming a thin (∼10 μm) immunoisolation layer protecting antibody-modified microbeads inside the capsule from immune cells on the outside. The microbeads were functionalized with antibodies against cytokines of interest: interferon (IFN)-γ and tumor necrosis factor (TNF)-α. While nonfouling, a hydrogel shell was permeable to cytokine molecules; these molecules were captured on microbeads and were detected with fluorescently labeled secondary antibodies. Calibration of encapsulated immunoassays with known concentrations of cytokines revealed a limit of detection of 14.8 and 14.4 pM for IFN-γ and TNF-α, respectively. We also demonstrated the concept of multicytokine detection by fabricating distinct populations of capsules carrying either anti-IFN-γ or anti-TNF-α microbeads and dispensing these capsules into a solution containing both cytokine types. Importantly, when placed into whole blood for 16 h, microcapsules were free of leukocytes, effectively protecting sensing beads from the blood components. To further demonstrate utility of this strategy, encapsulated microbeads were used for detection of IFN-γ in blood of patients with latent tuberculosis infection (LTBI) and unexposed healthy controls. When compared to gold standard technology (interferon gamma release assay or IGRA), our encapsulated immunoassay accurately predicted LTBI diagnosis in 11 out of 14 patients. Overall, encapsulation of immunoassays represents a promising strategy for keeping sensing elements operational in a highly fouling complex environment such as blood.

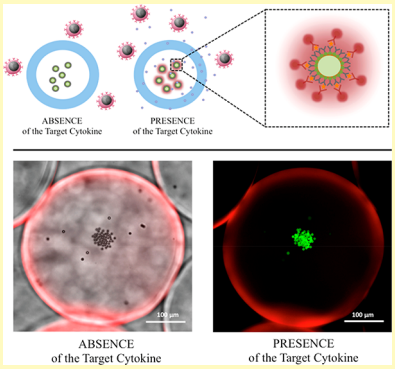


**KEYWORDS:** *microencapsulation, immunoassay, biosensor, interferon-γ, latent tuberculosis infection*



Ever since the demonstration of a glucose-selective electrode by Updike and Hicks in 1967,[1] the development of biosensors proceeded hand-in-glove with that of biological interfaces to ensure and extend biosensor operation in a fouling environment.[2] Over the years, sensing elements (e.g., enzymes) have been protected from the fouling biological environment by entrapment within polyacrylamide gels or by membranes or by polyelectrolyte coatings.[3−5] Poly(ethylene glycol) (PEG) hydrogels have been utilized extensively for minimizing fouling of biosensors.[6−9] For example, PEG hydrogel coatings have been used to improve the lifetime and operation of glucose-sensing electrodes developed by Heller and colleagues.[10] PEG hydrogels have also been fabricated into a variety of objects by photolithography or stop-flow lithography and have been loaded with biorecognition elements for biosensing applications.[11,12]

Droplet microfluidics represents another microfabrication approach that has been used for high-throughput cell encapsulation and biochemical assays.[13,14] Typically, droplet microfluidics devices produce water-in-oil emulsions, but this fabrication strategy can be adapted to produce hydrogel capsules.[15,16] The advantages of microfluidic fabrication include monodispersity of capsules size and also complexity of capsule composition.[17] For example, there have been reports of core−shell microcapsules produced using droplet microfluidics as miniaturized bioreactors for cultivation of yeast and mammalian cells.[18−20] Previously, our laboratory has reported on a strategy to fabricate microcapsules with an aqueous core

**Received:** September 13, 2018
**Accepted:** January 27, 2019




DOI: 10.1021/acssensors.8b01033
ACS Sens. XXXX, XXX, XXX−XXX

**Scheme 1. Sensing with Microcapsules**[a]

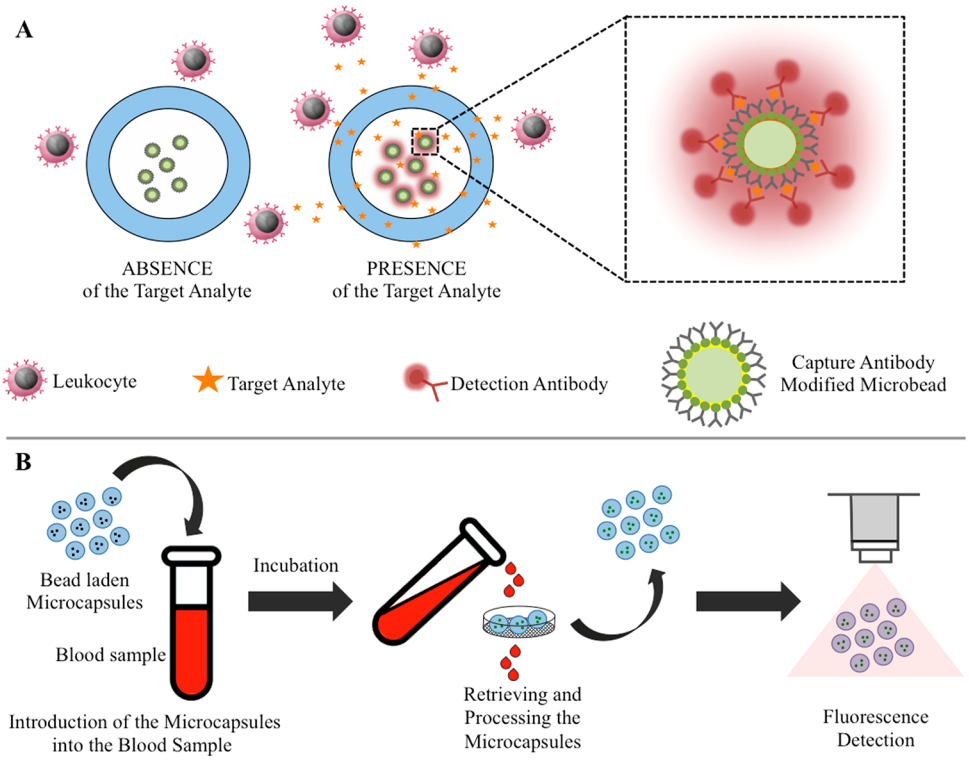


[a](A) Close-up view of microcapsules immersed in blood. Cytokines from stimulated leukocytes diffuse into the core of a microcapsule and are captured by antibody-modified beads residing in the core. Presence of the target analyte is revealed by staining with secondary fluorescently-labeled antibody. The fluorescence intensity of encapsulated microbeads correlates with concentration of cytokine in blood. (B) Workflow of detecting cytokine with sensing microcapsules. The microcapsules are added into a heparinized tube containing patient's blood and are incubated overnight under cell culture conditions. Upon completion of the incubation, the microcapsules are separated from the blood cells using a strainer with 40-200$\mu$m-mesh size. The microcapsules are then incubated with fluorescent secondary antibody and are imaged to quantify fluorescence intensity.

and hydrogel shell for entrapment of cells and formation of spheroids.[21] Here, we wanted to explore the use of core−shell microcapsules for entrapment of antibody-modified microbeads for detection of cytokines in blood.

Cytokines are released by immune cells responding to infections, malignancies, or autoimmune disorders.[22] Interferon (IFN)-$\gamma$ and TNF-$\alpha$ are some of the most common cytokines released by leukocytes. The former is of T-cell origin and may be indicative of T-cell response to antigenic stimulation, while the latter indicates a general inflammatory response and can be produced by a number of leukocyte subtypes, including T-cells and monocytes.[23,24] IFN-$\gamma$ is particularly important as a diagnostic marker of latent tuberculosis infection (LTBI), which is detected by either an ELISpot- or an ELISA-based interferon gamma release assay (IGRA).[25−27] However, both IGRAs are multistep assays that involve removal of blood cells followed by a complex multistep ELISpot or ELISA detection method.[28]

Our objective was to employ microcapsules carrying Ab-modified microbeads for detection of IFN-$\gamma$ and TNF-$\alpha$ in minimally processed blood. We reasoned that isolating sensing microbeads inside core−shell microcapsules will eliminate the need for multiple sample preparation steps and will allow us to sample cytokines in unprocessed blood (see Scheme 1). This paper describes our efforts to characterize encapsulated Ab-modified microbeads as immunosensors for detection of IFN-$\gamma$ and TNF-$\alpha$. As proof of concept, we assessed the utility of IFN-$\gamma$ sensing microcapsules for detection of IFN-$\gamma$ in patients with LTBI.

## MATERIALS AND METHODS

**Fabrication of Microfluidic Devices.** Droplet generating devices were fabricated as previously described.[21] Briefly, top and bottom masters were prepared by spin coating three layers of SU-8 photoresist (MicroChem, Westborough, MA) on a 4 in. silicon wafer (University Wafer, USA). The first layer (60 $\mu$m) was exposed to UV light through a photomask representing the core channel pattern. After postexposure bake, a second SU-8 layer (40 $\mu$m) was similarly spin coated and exposed through a second photomask corresponding to the shell channel pattern using a mask aligner (Kloe UV-KUB 3, France). The spin-coating and exposure steps were repeated for the oil channel layer (50 $\mu$m). Subsequently, a wafer was placed into a developer solution to remove photoresist regions not exposed to UV light. We found the process of three spin-coating and exposure steps followed by a single development step to be better than developing each layer, because cleaning the surface in preparation for the next layer could damage the former layer. PDMS (Ellsworth adhesive, Minneapolis, MN) was then poured over a silicon master and replica molded by standard soft lithography procedures. Cured "top" and "bottom" PDMS pieces were then treated with 40s of exposure to air plasma (G-500 plasma cleaning system, Yield Engineering Systems, Livermore, CA), and manually aligned under a stereoscope (Zeiss Stemi 508, Germany) using deionized water as a lubricating layer. Aligned chips were then placed on a hot plate at 95 °C for 4 h to remove the water layer and bond the two PDMS layers together. Subsequently, microfluidic devices were infused with an Aquapel solution to render surfaces hydrophobic in preparation for droplet generation. The final chip dimensions (height)


DOI: 10.1021/acssensors.8b01033
ACS Sens. XXXX, XXX, XXX−XXX

were a 120 $\mu$m core channel, 200 $\mu$m shell channel, and 300 $\mu$m oil channel (Figure 1A and Supporting Information Figure S1).

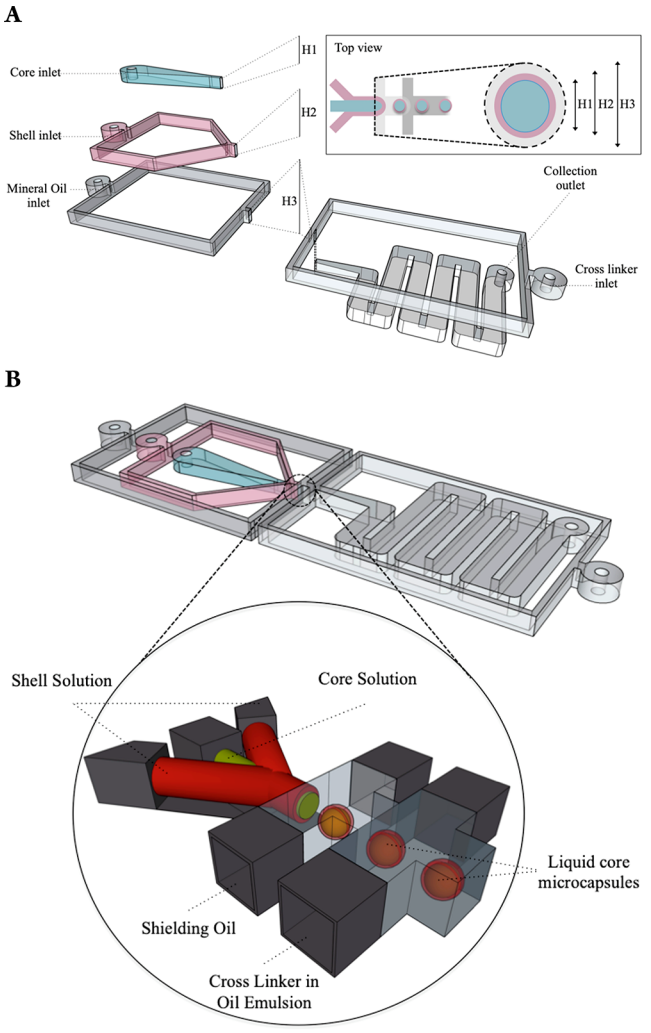


**Figure 1.** Fabrication of core−shell microcapsules. (A) Description of the microfluidic device. The droplet generator is composed of four inlet channels and a serpentine that leads to droplet collection port. The core, shell, and oil channels have heights of 120 $\mu$m (H1), 200 $\mu$m (H2), and 300 $\mu$m (H3), respectively. The top view panel describes how channels of different dimensions correlate to the core and shell components of microcapsules. B) A 3D rendering to help visualize the process of fabricating core−shell microcapsules. The core flow stream contains beads, high molecular weight PEG and a Densifier. The shell stream contains cross-linkable 4Arm PEG-Maleimide (Mal). Upon ejection from the nozzle into the oil phase, the liquid in the shell wraps around the material in the core. Subsequently, PEG-4Mal in the shell forms a gel after interaction with oil/cross-linker stream. Large molecular weight PEG molecules lacking functional groups diffuse out of the core and are replaced by aqueous environment within an hour of capsule fabrication.

**Microfluidic Device Operation and Capsule Fabrication.** Microfluidic coaxial flow-focusing devices were infused with 4 different solutions to generate capsules: (1) a core solution composed of 16% w/v PEG (35 kDa) and 50% Optiprep densifier (Sigma-Aldrich, St. Louis, MO) dissolved in desired cell culture media containing capture beads, (2) a shell solution containing 4−8% w/v 4-arm maleimide functionalized polyethylene glycol (PEG4MAL, Creative PEGwork, Durham, NC) and 15 mM triethanolamine (TEA) dissolved in the same media, (3) a shielding organic phase of mineral oil with 0.5% v/v Span-80 surfactant, and (4) a cross-linking organic phase of mineral oil with 3% Span-80 and a 1:15 emulsion of 25 mg/mL dithiothrietol (DTT) (Sigma-Aldrich, St. Louis, MO) dissolved in DI water (emulsion was generated by sonicating oil/water mixture for 30 min in an ultrasonic bath). Each of the four solutions was filtered through 0.2 $\mu$m centrifuge filters and loaded into syringes under sterile conditions. Following this sterilization step, core, shell, shielding oil, and cross-linking solutions were infused into separate inlets (see Figure 1B) of a microfluidic device using syringe pumps (Harvard Apparatus, Holliston, MA) at flow rates of 3−5 $\mu$L·min$^{-1}$ for core, 3−5 $\mu$L·min$^{-1}$ for shell, 30−40 $\mu$L·min$^{-1}$ for shielding oil, and 40−60 $\mu$L·min$^{-1}$ for cross-linking oil. Pushing the aqueous mixture of core and shell solutions through an orifice into the oil phase resulted in formation of droplets that retained their shape prior to gelation. Upon addition of the dithiolated cross-linker (DTT) through the fourth stream, PEG4Mal molecules in the shell become cross-linked forming a gel layer (see Supporting Information Movies S1 and S2). These capsules are collected into an Eppendorf tube containing 1% BSA in PBS. The capsules reside in the oil phase layer above the aqueous layer in the tube and slowly partition into the liquid phase. Mechanical agitation expedites the transfer of capsules from oil to aqueous phase.

*Preparation of Antibody-Functionalized Microbeads.* Streptavidin-coated microbeads (Spherotech, Lake Forest, IL) were used for detection of cytokines in our experiments. Biotinylated anti-IFN-$\gamma$ and anti-TNF-$\alpha$ Abs were immobilized on microbeads (5−5.9 $\mu$m diameter) according to protocols described by us previously.[29,30] Briefly, prior to functionalization, microbeads were incubated with Pierce protein-free blocking buffer (ThermoFisher Scientific, Grand Island, NY) for 2 h at 4 °C, and then washed with PBS via centrifugation (13,000 rcf, 5 min). In the next step, 50 $\mu$L of streptavidin microbeads (~3.6 × 106 beads) was incubated with 5 $\mu$g of biotinylated capture Abs (R&D systems, Minneapolis, MN) in 250 $\mu$L of 1% BSA in PBS overnight at 4 °C. For quantifying the number of antibodies per bead, we estimate this number to be ~5 × 10$^6$ Ab molecules/beads. This estimate is based on the formula shown below:

$$\text{antibodies/bead} = \frac{A}{K} = \frac{2\pi r^2}{47.1} \approx 1.66 \times 10^6$$

where $A$ is the surface area of a bead and $K$ represents the IgG footprint (nm$^2$). The surface area for porous polystyrene beads was reported by the manufacturer to be 7.8 × 10$^7$ nm$^2$ (Spherotech Inc., Lake Forest, IL). The footprint for antibody molecule is ~31.4−62.8 nm$^2$.[31] Based on these parameters we estimated the loading capacity of one bead to be ~1.66 × 10$^6$ Ab molecules. Given that the total number of beads to be functionalized with Abs was ~3.6 × 10$^6$ per batch we incubated the beads with 5 $\mu$g (≈20 × 10$^{12}$ molecules) of Ab. After Ab immobilization, microbeads were washed in PBS by centrifugation before reconstituting in 2× concentrated core solution. The microbeads were encapsulated according to the protocol described above. Encapsulated microbeads were stable at 4 °C in the dark for up to 2 weeks (see Figure S2).

*Detecting TNF-α and IFN-γ Using Encapsulated Microbeads.* Sandwich immunoassay was used to detect capture of cytokine molecules on microbeads. Secondary Abs, polyclonal human anti-IFN-$\gamma$ and anti-TNF-$\alpha$ (R&D systems, Minneapolis, MN), were labeled with Alexa-488 and Alexa-546, respectively, using commercial kits and following manufacturer's instructions (ThermoFisher Scientific, Grand Island, NY).

For microcapsule visualization, 1 $\mu$g/mL of thiolated dye (Rhodamin/FITC/Cy5)/PEG conjugate (SH-PEG-dye 5 kDa) (Creative PEGwork, Durham, NC) was included in the shell solution along with 15 mM TEA. The latter chemical was used to reduce thiol groups and enhance uniformity of dye conjugation within the gel.

In order to establish figures of merit (limit of detection and linear range), encapsulated microbeads were challenged with different concentrations of recombinant IFN-$\gamma$ and TNF-$\alpha$ (R&D systems, Minneapolis, MN). After 2 h incubation with recombinant cytokines, microcapsules were labeled by 2 h exposure to fluorescently labeled secondary Abs and then imaged with fluorescence microscope


DOI: 10.1021/acssensors.8b01033
ACS Sens. XXXX, XXX, XXX−XXX

(Olympus IX 83, Tokyo, Japan). Calibration curves of fluorescence intensity vs cytokine concentration were constructed with the aid of image analysis software (ImageJ2 ver. 1.51u).

**Blood Sample Collection and Processing.** The study was approved by the Mayo Clinic Institutional Review Board (IRB#: 09-003253). All study participants signed an informed written consent and were enrolled between August 2017 and December 2017. Study subjects included unexposed individuals with negative QuantiFERON-TB Gold In-Tube (QFT) results and subjects with LTBI diagnosis as per current guidelines criteria, including asympto- matic subjects at risk of prior tuberculosis (TB) exposure, negative chest X-rays, and by prior positive QFT results as previously described.[32,33] Each blood sample was collected into three 1 mL QFT tubes (Qiagen, Germantown, MD) labeled "Mitogen", "Antigen", and "Nil", representing the positive control, antigen peptide mixture, and negative control samples, respectively. QFT was performed as recommended by the manufacturer. A cutoff level of IFN-$\gamma \geq 0.35$ IU/mL and >50% above nil defined a QFT(+) test. Research laboratory technicians were blinded to the results of QFT. Approximately 125 sensing microcapsules were added into each tube and were incubated overnight at 37 °C with 5% $CO_2$ on a shaker operating at 131 rpm. After incubation in blood, microcapsules were retrieved using 37 $\mu$m cell strainers (Stemcell technologies, Vancouver, Canada) and were then stained with fluorescently labeled detection Abs for 2 h at room temperature. After staining, microcapsules were washed with 1% BSA in PBS and visualized using a fluorescence microscope (Olympus IX 83, Tokyo, Japan). On-bead fluorescence intensity was analyzed using ImageJ2 software.

Peripheral blood mononuclear cells (PBMCs) were also used in some of the calibration experiments. These cells were isolated in the Mayo Clinic transfusion medicine component laboratory as reported previously.[34] PMA (phorbol 12-myristate-13-acetate) and ionomycin (Sigma-Aldrich, St. Louis, MO) stimulation was carried out using 100 ng/mL PMA and 1 $\mu$g/mL ionomycin.

**Statistical Analysis.** Data are represented as mean ± SEM. Statistical significance between experimental groups was assessed using a two-tailed student's $t$ test and $p$-values < 0.05 or in some cases <0.01 were considered statistically significant.

## RESULTS AND DISCUSSION

The objective of this paper was to explore utility of encapsulated microbeads for detection of cytokines in human blood. We demonstrate that such microcapsules can be used for sensitive measurements of IFN-$\gamma$ and TNF-$\alpha$ and for diagnosis of LTBI.

**Fabrication of Sensing Microcapsules.** Sensing capsules were fabricated using droplet microfluidics to contain a hydrogel shell and an aqueous core with free-floating Ab-modified microbeads. The shell thickness is controlled in part by the relative flow rates of core and shell solutions. We wanted to minimize shell thickness to ensure rapid and unimpeded diffusion of cytokines and secondary Abs. The flow rate of 4 $\mu$L.min$^{-1}$ for both core and shell solutions resulted in a hydrogel shell of ~10 $\mu$m and was chosen for our fabrication process. Importantly, despite a relatively thin shell, microcapsules remained mechanically stable and were not broken during a series of sequential vortex (~250 rpm)/steady cycles.

Additionally, in order to investigate the diffusion of secreted cytokines through the shell and into the core where the sensing beads were situated, we loaded the microcapsules with fluorescent molecules (20 kDa Dextran-Alexa-546) similar in the size to IFN-$\gamma$ and TNF-$\alpha$ and monitored fluorescence over time. As can be seen from Figure S3, after ~40 min, fluorescence signals inside and outside capsules became similar. These experiments demonstrated that porosity of the hydrogel shell of microcapsules was sufficient for diffusion of cytokines.

**Optimizing Microcapsule Numbers to Ensure Sensitive Detection of Cytokines.** Fluorescence signal in microcapsules may depend not only on the concentration of cytokines in the sample but also on the number of Ab-binding sites in the sample. There are different strategies for controlling the number of Ab sites (1) by adjusting Ab concentration during bead functionalization, (2) by controlling the number of encapsulated microbeads, and (3) by controlling the number of microcapsules present in the sample. We opted to maximize the number of Ab molecules per bead to increase the possibility of target analyte capture. In parallel, we selected the number of sensing beads per capsule by running a series of experiments with different population sizes of the beads. Considering that the range of Poisson-distributed beads varied by about ±20 beads per capsule, we aimed for ~50 beads per capsule as an optimal condition that would result in a sufficient number of beads for analysis of cytokine binding. As result, we focused on scenario (3), optimizing the number of capsules per sample. In this experiment, different numbers of microcapsules (ranging from 125 to 1000) were placed into 1 mL of 1% BSA solution containing 14 pM concentration of IFN-$\gamma$ for 16 h and then stained with detection Abs. Results shown in Figure S4 reveal that the average fluorescence from a sample containing 125 microcapsules was significantly higher than the intensity from samples containing a larger number of capsules. Therefore, we chose to work with ~100 microcapsules per 1 mL sample. Using fewer than 100 microcapsules was impractical, since it was difficult to isolate/filter a small number capsules prior to staining with secondary Abs and fluorescence detection.

DTT, the cross-linker used to create a hydrogel shell during the droplet fabrication process, has been reported to affect functionality of Abs.[35,36] To check whether Abs immobilized on microbeads was affected by this reagent, we compared two populations of microcapsules: (1) microcapsules with Ab-functionalized microbeads exposed to DTT during microfluidic fabrication, and (2) microcapsules with avidin-functionalized microbeads that were exposed to biotinylated Abs post encapsulation. As shown by data in Figure S5, both populations of microcapsules exhibited similar fluorescence intensity after challenge with 57.5 pM (1 ng/mL) TNF-$\alpha$. This suggested that microfluidic fabrication of capsules did not affect functionality of capture Abs.

**Characterizing Responses of Microcapsules to Known Concentrations of IFN-$\gamma$ and TNF-$\alpha$.** Calibration curves were constructed to establish a relationship between fluorescence intensity and cytokine concentrations. For these experiments, we placed microcapsules into test solutions containing different concentrations of IFN-$\gamma$ or TNF-$\alpha$, in the range of 0 to 250 pM. This concentration range was selected based on the reported levels of these cytokines in blood.[37] Staining with fluorescently labeled detection Abs revealed that on-bead fluorescence signal varied depending on the concentration of recombinant cytokines (see Figure S6). Calibration curves presented in Figure 2A,B demonstrate that the response in sensing microcapsules remained linear for the concentration range tested. Our results demonstrate that fluorescence intensity associated with the lowest concentration of IFN-$\gamma$ and TNF-$\alpha$ tested, 14 pM, was significantly higher than the control sample without cytokine ($P$-value < 0.05). This is comparable to other previously reported fluorescence


DOI: 10.1021/acssensors.8b01033
ACS Sens. XXXX, XXX, XXX−XXX

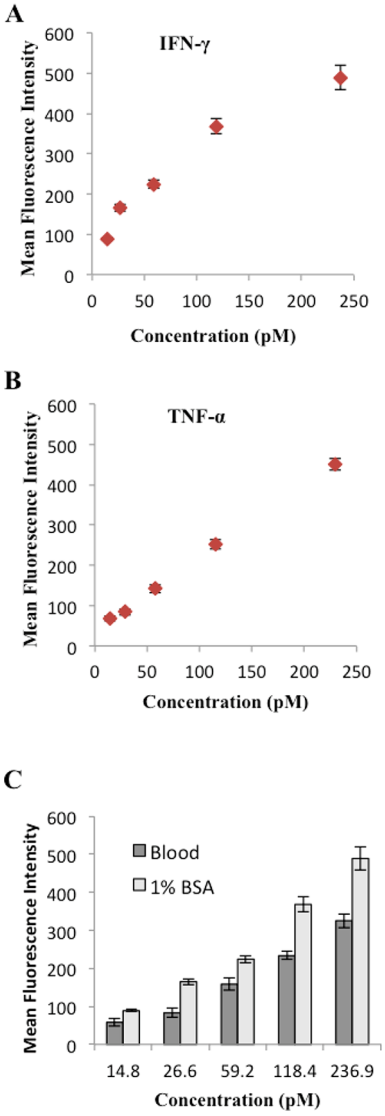


**Figure 2.** Characterization of microcapsules for detection of IFN-$\gamma$ and TNF-$\alpha$. (A) Calibration curve constructed by exposure of sensing microcapsules to concentrations of IFN-$\gamma$ varying from 14 pM (250 pg/mL) to 236 pM (4 ng/mL). (B) Calibration curve for TNF-$\alpha$ constructed by exposure of sensing microcapsules to concentrations ranging from 14 to 230 pM (250 pg/mL to 4 ng/mL). Both calibration curves were constructed by measuring mean fluorescent intensity of the encapsulated beads after 120 min of incubation with known concentrations of analyte ($n$ = 12, $p$ < 0.05). (C) Detecting recombinant IFN-$\gamma$ in1% BSA in PBS) as well as in whole blood after 16 h incubation at 37 °C with 5% $CO_2$. Concentration range tested from 14 to 236 pM. BSA, bovine serum albumin; scale bar is 200 $\mu$m.

immunoassays without signal amplification.[38−40] Another commonly used method is to set a limit of detection as a signal 3x greater than noise. Based on this method, our limit of detection is ∼9 and ∼5 pM for IFN-$\gamma$ and TNF-$\alpha$, respectively.

Furthermore, in order to verify the performance of the biosensor in a fouling environment, the microcapsules were incubated overnight in blood with spiked concentrations of recombinant INF-$\gamma$. As shown in Figure 2C, the fluorescence signal from sensing microbeads correlated with different concentrations of target cytokine. The difference (25−30%) in signals obtained from1% BSA solution and whole blood may be attributed to a much more complex composition of the latter. Leukocytes in blood may uptake cytokines including IFN-$\gamma$, or there may also be proteases in blood that digest cytokines contributing to a lower detected signal. We should note that microcapsules extracted from blood after overnight incubation at 37 °C remained free of leukocytes (see Figure 3A,B). Therefore, leukocyte adhesion did not result in a barrier to cytokine transport and did not contribute to lower signals detected in blood (Figure 3C).

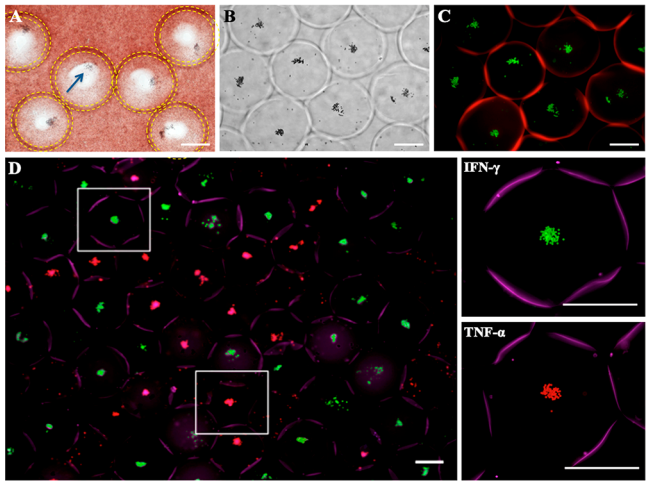


**Figure 3.** Sensing microcapsules in action. (A) Microcapsules in a fouling environment (whole blood). The yellow dotted double line indicates the shell of microcapsules. The arrow points to the beads that are settled in the core. (B) Recovered microcapsules after overnight incubation with stimulated blood at 37 °C. (C) INF- $\gamma$ signal on sensing beads (green) in the core of the same capsules with Rhodamine labeled hydrogel shell (red). (D) Dual cytokine detection using a mixed population of microcapsules containing IFN-$\gamma$ and TNF-$\alpha$ specific microbeads. Microcapsules were incubated with a mixture of 60 pM IFN-$\gamma$ and TNF-$\alpha$ and then exposed to anti-IFN-$\gamma$ Alexa 488 (green) and anti-TNF-$\alpha$ Alexa 546 (red). The scale bar is 200 $\mu$m.

**Simultaneous Detection of IFN-$\gamma$ and TNF-$\alpha$ in the Same Sample.** Microcapsule-based immunoassays are amenable to multiplexed detection of cytokines. Several routes for multiplexing can be envisioned, for example, by labeling the hydrogel shell with different fluorescent dyes or by utilizing detection Abs with different fluorophore labels. For a proof-of-concept experiment, we fabricated two populations of microcapsules, one containing anti-TNF-$\alpha$ microbeads and the second containing anti-IFN-$\gamma$ beads, and then placed microcapsules into a test sample containing 60 pM IFN-$\gamma$ and TNF-$\alpha$. Staining with detection Abs, anti-IFN-$\gamma$ Alexa 488 (green), and anti-TNF-$\alpha$ Alexa 546 (red) revealed green and red fluorescence signal from IFN-$\gamma$ and TNF-$\alpha$ sensing microcapsules, respectively (Figure 3D). Using calibration curves described in Figure 2, fluorescence intensity was converted into concentration, 62.32 pM IFN-$\gamma$ and 57.01 pM TNF-$\alpha$. These values were similar to the initial concentration of cytokines spiked into the solution.

We also tested performance of microcapsules for detection of IFN-$\gamma$ and TNF$\alpha$ in buffers containing one or both of these cytokines. Figure S7 highlights the fact that a fluorescence signal was observed from the correct set of microcapsules in the presence of the correct cytokine. No cross-reactivity


DOI: 10.1021/acssensors.8b01033
ACS Sens. XXXX, XXX, XXX−XXX

between Ab-modified microbeads or off-target capture of incorrect cytokines was observed in the microcapsules.

**Comparison of the Sensing Microcapsules with ELISA from the IGRA Method for the Diagnosis of LTBI.** In order to further validate this technology, we compared the sensing microcapsules with the QFT method to detect IFN-$\gamma$ in whole blood samples from 5 QFT(+) patients with LTBI diagnosis and 9 unexposed controls. To that end, we utilized the QFT platform to obtain whole blood samples incubated with the specific *M. tuberculosis* antigen peptide mixtures and controls to compare the utility of the sensing microcapsules to detect IFN-$\gamma$ levels and utilized the ELISA method of the QFT assay as a gold standard comparison. The workflow of this experiment is shown in Schematic 1B. Microcapsules were placed into QFT tubes marked as Mitogen, Antigen, or Nil were incubated in whole unprocessed blood. Stimulation of leukocytes and production of IFN-$\gamma$ was expected to occur in the tubes during the 16h incubation. Microcapsules were then recovered and characterized using fluorescence microscopy. Importantly, we observed limited to no cell attachment to microcapsules, suggesting that PEG hydrogel shells were effective in eliminating fouling.[41] An analysis of 14 study subject samples revealed that our technology was accurate in delivering correct diagnosis in 11 out of 14 cases (see Table 1). To achieve diagnosis for the sensing microcapsules, we used criteria for positive, negative, and intermediate results as outlined in Table S1. Figure 4 shows representative signals from microcapsules incubated with QFT (+) and QFT (−) samples.

We should note that all three cases of incorrect diagnosis for our technology were false negatives in samples with low levels of IFN-$\gamma$ (<10 pM). This outlines the need to decrease the limit of detection for sensing microcapsules down to 1 pM.

This improved limit of detection may be achieved in the future by incorporating enzymatic signal amplification inside microcapsules. Despite limited sensitivity for detecting LTBI with low levels of IFN-$\gamma$, the concept of encapsulated immunoassays holds significant promise for sensing/sampling composition of complex biological fluids such as blood. In this paper, use of microcapsules with a nonfouling hydrogel shell allowed detection in undiluted whole blood and obviated the need for blood separation steps that typically precede cytokine sensing.

**Table 1. Comparison of Results of Study Subjects Between the IGRA (Gold Standard) and Sensing Microcapsule**

| Case # | IGRA | Biosensor |
|---|---|---|
| 1 | Negative | Negative |
| 2 | Positive | Negative |
| 3 | Negative | Negative |
| 4 | Positive | Positive |
| 5 | Negative | Negative |
| 6 | Negative | Negative |
| 7 | Negative | Negative |
| 8 | Negative | Negative |
| 9 | Negative | Negative |
| 10 | Positive | Negative |
| 11 | Negative | Negative |
| 12 | Negative | Negative |
| 13 | Positive | Intermediate |
| 14 | Positive | Positive |

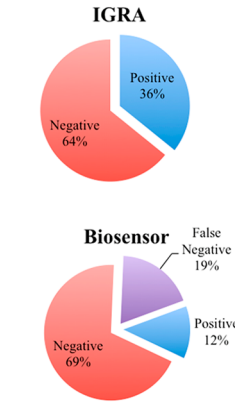


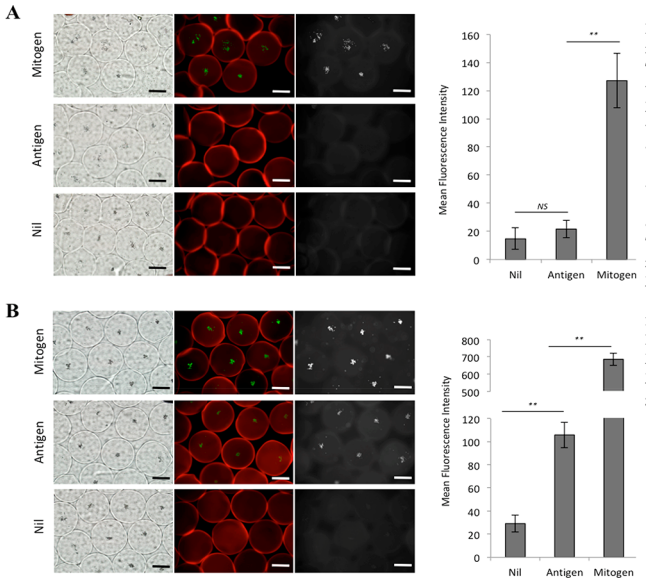


**Figure 4.** Representative results from patients suspected of latent TB infection. (A) Sample that tested negative for LTBI and (B) sample that tested positive for positive for LTBI. The shell of the capsules is labeled with Rhodamine (red fluorescent), and anti-IFN-$\gamma$ is conjugated to Alexa-488 (green). Green fluorescence indicates presence of IFN-$\gamma$ in the blood sample. The fluorescence images converted into binary (black and white), and MFIs were measured using ImageJ ($n$ = 12, $^{**}p < 0.01$). The scale bar is 200 $\mu$m. LTBI, late tuberculosis infection; IFN-$\gamma$, interferon-$\gamma$; MFI, mean fluorescence intensity; mitogen, positive control; antigen, test; nil, negative control.

## CONCLUSIONS

In this work, we developed microcapsules incorporating sensing microbeads for detection of cytokines in human blood. Microcapsules are fabricated using droplet microfluidics to contain a hydrogel shell and aqueous core. Ab-modified microbeads are entrapped in the aqueous core and isolated from the leukocytes in the blood by the hydrogel shell. Thus, microcapsules function as sampling units capturing cytokine molecules on Ab-modified microbeads. Detection of IFN-$\gamma$ and TNF-$\alpha$ was accomplished by collecting microcapsules from blood followed by staining with secondary fluorescent Abs. This staining revealed a limit of detection of ~14 pM for IFN-$\gamma$ and TNF-$\alpha$. Importantly, we tested IFN-$\gamma$ levels in 14 blood samples from patients with LTBI and unexposed controls and demonstrated ~80% concordance between encapsulated immunoassay and a gold standard technology (QFT). Moving forward, we envision developing single-step in-capsule detection strategies to simplify this assay. We also foresee developing microcapsules carrying different sensing microbeads for multiplexed detection of cytokines in blood.

## ASSOCIATED CONTENT

### Supporting Information

The Supporting Information is available free of charge on the ACS Publications website at DOI: 10.1021/acssensors.8b01033.

Data supporting the conclusions and additional clarification for the microfluidic fabrication methods (PDF)

Core−shell microcapsule fabrication, general view of all the channels (AVI)



DOI: 10.1021/acssensors.8b01033
ACS Sens. XXXX, XXX, XXX−XXX

Core−shell microcapsule formation at the aqueous−oil interface (AVI)

## AUTHOR INFORMATION


### Corresponding Author

*E-mail: revzin.alexander@mayo.edu.

### ORCID

Ali Rahimian: 0000-0003-3263-7789

Alexander Revzin: 0000-0002-8737-3250


### Author Contributions

All authors have given approval to the final version of the manuscript.

### Notes

The authors declare no competing financial interest.

## ACKNOWLEDGMENTS

We would like to thank Debra Nesler at Mayo Clinic Pulmonary Research Unit for her efforts in coordinating with patients in order to collect blood samples. We thank members of the Revzin Laboratory for their insightful comments and feedback. This work was supported in part by a NIH grant (AI121779-01).

## ABBREVIATIONS

PEG, polyethylene glycol; IFN-$\gamma$, interferon-$\gamma$; TNF-$\alpha$, tumor necrosis factor-$\alpha$; LTBI, latent tuberculosis infection

## REFERENCES


(1) Updike, S. J.; Hicks, G. P. The enzyme electrode. *Nature* **1967**, *214*, 986−8.

(2) Rocchitta, G.; Spanu, A.; Babudieri, S.; Latte, G.; Madeddu, G.; Galleri, G.; Nuvoli, S.; Bagella, P.; Demartis, M. I.; Fiore, V.; Manetti, R.; Serra, P. A. Enzyme Biosensors for Biomedical Applications: Strategies for Safeguarding Analytical Performances in Biological Fluids. *Sensors* **2016**, *16*, 780.

(3) Sassolas, A.; Blum, L. J.; Leca-Bouvier, B. D. Immobilization strategies to develop enzymatic biosensors. *Biotechnol. Adv.* **2012**, *30*, 489−511.

(4) Kim, J. H.; Choi, D. C.; Yeon, K. M.; Kim, S. R.; Lee, C. H. Enzyme-Immobilized Nanofiltration Membrane To Mitigate Biofouling Based on Quorum Quenching. *Environ. Sci. Technol.* **2011**, *45*, 1601−7.

(5) Ambrózy, A.; Hlavatá, L.; Labuda, J. Protective membranes at electrochemical biosensors. *Acta Chimica Slovaca* **2013**, *6*, 35−41.

(6) Matharu, Z.; Enomoto, J.; Revzin, A. Miniature Enzyme-Based Electrodes for Detection of Hydrogen Peroxide Release from Alcohol-Injured Hepatocytes. *Anal. Chem.* **2013**, *85*, 932−9.

(7) Yan, J.; Pedrosa, V. A.; Enomoto, J.; Simonian, A. L.; Revzin, A. Electrochemical biosensors for on-chip detection of oxidative stress from immune cells. *Biomicrofluidics* **2011**, *5*, 032008.

(8) Koh, W. G.; Pishko, M. Immobilization of multi-enzyme microreactors inside microfluidic devices. *Sens. Actuators, B* **2005**, *106*, 335−42.

(9) Yan, J.; Pedrosa, V. A.; Simonian, A. L.; Revzin, A. Immobilizing Enzymes onto Electrode Arrays by Hydrogel Photolithography to Fabricate Multi-Analyte Electrochemical Biosensors. *ACS Appl. Mater. Interfaces* **2010**, *2*, 748−55.

(10) Ohara, T. J.; Rajagopalan, R.; Heller, A. Wired Enzyme Electrodes for Amperometric Determination of Glucose or Lactate in the Presence of Interfering Substances. *Anal. Chem.* **1994**, *66*, 2451−7.

(11) Shin, D. S.; Liu, Y.; Gao, Y. D.; Kwa, T.; Matharu, Z.; Revzin, A. Micropatterned Surfaces Functionalized with Electroactive Peptides for Detecting Protease Release from Cells. *Anal. Chem.* **2013**, *85*, 220−227.

(12) Le Goff, G. C.; Srinivas, R. L.; Hill, W. A.; Doyle, P. S. Hydrogel microparticles for biosensing. *Eur. Polym. J.* **2015**, *72*, 386−412.

(13) Huang, H. S.; Yu, Y.; Hu, Y.; He, X. M.; Usta, O. B.; Yarmush, M. L. Generation and manipulation of hydrogel microcapsules by droplet-based microfluidics for mammalian cell culture. *Lab Chip* **2017**, *17*, 1913−32.

(14) Shang, L. R.; Cheng, Y.; Zhao, Y. J. Emerging Droplet Microfluidics. *Chem. Rev.* **2017**, *117*, 7964−8040.

(15) Guillot, P.; Colin, A. Stability of parallel flows in a microchannel after a T junction. *Phys. Rev. E* **2005**, *72*, 066301.

(16) Siltanen, C.; Yaghoobi, M.; Haque, A.; You, J.; Lowen, J.; Soleimani, M.; Revzin, A. Microfluidic fabrication of bioactive microgels for rapid formation and enhanced differentiation of stem cell spheroids. *Acta Biomater.* **2016**, *34*, 125−32.

(17) Headen, D. M.; Aubry, G.; Lu, H.; Garcia, A. J. Microfluidic-Based Generation of Size-Controlled, Biofunctionalized Synthetic Polymer Microgels for Cell Encapsulation. *Adv. Mater.* **2014**, *26*, 3003−8.

(18) Ekanem, E. E.; Zhang, Z.; Vladisavljevic, G. T. Facile microfluidic production of composite polymer core-shell microcapsules and crescent-shaped microparticles. *J. Colloid Interface Sci.* **2017**, *498*, 387−94.

(19) Agarwal, P.; Zhao, S. T.; Bielecki, P.; Rao, W.; Choi, J. K.; Zhao, Y.; Yu, J.; Zhang, W.; He, X. One-step microfluidic generation of pre-hatching embryo-like core-shell microcapsules for miniaturized 3D culture of pluripotent stem cells. *Lab Chip* **2013**, *13*, 4525−33.

(20) Kim, C.; Chung, S.; Kim, Y. E.; Lee, K. S.; Lee, S. H.; Oh, K. W.; Kang, J. Y. Generation of core-shell microcapsules with three-dimensional focusing device for efficient formation of cell spheroid. *Lab Chip* **2011**, *11*, 246−52.

(21) Siltanen, C.; Diakatou, M.; Lowen, J.; Haque, A.; Rahimian, A.; Stybayeva, G.; Revzin, A. One step fabrication of hydrogel microcapsules with hollow core for assembly and cultivation of hepatocyte spheroids. *Acta Biomater.* **2017**, *50*, 428−36.

(22) Chung, K. F. *Cytokines. Asthma and Copd: Basic Mechanisms and Clinical Management*, 2nd ed.; Academic Press, 2009; pp 327−341.

(23) Cavalcanti, Y. V.; Brelaz, M. C.; Neves, J. K.; Ferraz, J. C.; Pereira, V. R. Role of TNF-Alpha, IFN-Gamma, and IL-10 in the Development of Pulmonary Tuberculosis. *Pulm. Med.* **2012**, *2012*, 745483.

(24) Sasiain, M. C.; de la Barrera, S.; Fink, S.; Finiasz, M.; Aleman, M.; Farina, M. H.; Pizzariello, G.; Valdez, R. Interferon-gamma (IFN-gamma) and tumour necrosis factor-alpha (TNF-alpha) are necessary in the early stages of induction of CD4 and CD8 cytotoxic T cells by Mycobacterium leprae heat shock protein (hsp) 65 kD. *Clin. Exp. Immunol.* **1998**, *114*, 196−203.

(25) Chee, C. B.; KhinMar, K. W.; Gan, S. H.; Barkham, T. M.; Pushparani, M.; Wang, Y. T. Latent tuberculosis infection treatment and T-cell responses to Mycobacterium tuberculosis-specific antigens. *Am. J. Respir. Crit. Care Med.* **2007**, *175*, 282−7.

(26) Leem, A. Y.; Song, J. H.; Lee, E. H.; Lee, H.; Sim, B.; Kim, S. Y.; Chung, K. S.; Kim, E. Y.; Jung, J. Y.; Park, M. S.; Kim, Y. S.; Chang, J.; Kang, Y. A. Changes in cytokine responses to TB antigens ESAT-6, CFP-10 and TB 7.7 and inflammatory markers in peripheral blood during therapy. *Sci. Rep.* **2018**, *8*, 1159.

(27) Pai, M.; Denkinger, C. M.; Kik, S. V.; Rangaka, M. X.; Zwerling, A.; Oxlade, O.; Metcalfe, J. Z.; Cattamanchi, A.; Dowdy, D. W.; Dheda, K.; Banaei, N. Gamma interferon release assays for detection of Mycobacterium tuberculosis infection. *Clin Microbiol Rev.* **2014**, *27*, 3−20.

(28) Lalvani, A. Diagnosing tuberculosis infection in the 21st century: new tools to tackle an old enemy. *Chest* **2007**, *131*, 1898−906.

(29) Son, K. J.; Rahimian, A.; Shin, D. S.; Siltanen, C.; Patel, T.; Revzin, A. Microfluidic compartments with sensing microbeads for dynamic monitoring of cytokine and exosome release from single cells. *Analyst* **2016**, *141*, 679−88.




DOI: 10.1021/acssensors.8b01033
*ACS Sens.* XXXX, XXX, XXX−XXX

(30) Son, K. J.; Gheibi, P.; Stybayeva, G.; Rahimian, A.; Revzin, A. Detecting cell-secreted growth factors in microfluidic devices using bead-based biosensors. *Microsyst Nanoeng* **2017**, *3*, 17025.
(31) Chen, Y.; Cai, J.; Xu, Q.; Chen, Z. W. Atomic force bioanalytics of polymerization and aggregation of phycoerythrin-conjugated immunoglobulin G molecules. *Mol. Immunol.* **2004**, *41*, 1247−52.
(32) Escalante, P.; Peikert, T.; Van Keulen, V. P.; Erskine, C. L.; Bornhorst, C. L.; Andrist, B. R.; McCoy, K.; Pease, L. R.; Abraham, R. S.; Knutson, K. L.; Kita, H.; Schrum, A. G.; Limper, A. H. Combinatorial Immunoprofiling in Latent Tuberculosis Infection. Toward Better Risk Stratification. *Am. J. Respir. Crit. Care Med.* **2015**, *192*, 605−17.
(33) Lewinsohn, D. M.; Leonard, M. K.; LoBue, P. A.; Cohn, D. L.; Daley, C. L.; Desmond, E.; Keane, J.; Lewinsohn, D. A.; Loeffler, A. M.; Mazurek, G. H.; O'Brien, R. J.; Pai, M.; Richeldi, L.; Salfinger, M.; Shinnick, T. M.; Sterling, T. R.; Warshauer, D. M.; Woods, G. L. Official American Thoracic Society/Infectious Diseases Society of America/Centers for Disease Control and Prevention Clinical Practice Guidelines: Diagnosis of Tuberculosis in Adults and Children. *Clin. Infect. Dis.* **2017**, *64*, 111−5.
(34) Dietz, A. B.; Bulur, P. A.; Emery, R. L.; Winters, J. L.; Epps, D. E.; Zubair, A. C.; Vuk-Pavolovic, S. A novel source of viable peripheral blood mononuclear cells from leukoreduction system chambers. *Transfusion* **2006**, *46*, 2083−9.
(35) Hutterer, K. M.; Hong, R. W.; Lull, J.; Zhao, X. Y.; Wang, T.; Pei, R.; Le, M. E.; Borisov, O.; Piper, R.; Liu, Y. D.; Petty, K.; Apostol, I.; Flynn, G. C. Monoclonal antibody disulfide reduction during manufacturing Untangling process effects from product effects. *Mabs-Austin* **2013**, *5*, 608−13.
(36) Crivianu-Gaita, V.; Romaschin, A.; Thompson, M. High efficiency reduction capability for the formation of Fab antibody fragments from F(ab)2 units. *Biochem Biophys Rep* **2015**, *2*, 23−8.
(37) Liu, Y.; Rahimian, A.; Krylyuk, S.; Vu, T.; Crulhas, B.; Stybayeva, G.; Imanbekova, M.; Shin, D. S.; Davydov, A.; Revzin, A. Nanowire Aptasensors for Electrochemical Detection of Cell-Secreted Cytokines. *ACS Sens* **2017**, *2*, 1644−52.
(38) Giljohann, D. A.; Mirkin, C. A. Drivers of biodiagnostic development. *Nature* **2009**, *462*, 461−4.
(39) Yager, P.; Edwards, T.; Fu, E.; Helton, K.; Nelson, K.; TAM, M. R.; Weigl, B. H. Microfluidic diagnostic technologies for global public health. *Nature* **2006**, *442*, 412−8.
(40) Zhou, F. D.; Ding, F.; Chen, H.; Ding, W.; Zhang, W.; Chou, S. Y. Enhancement of Immunoassay's Fluorescence and Detection Sensitivity Using Three-Dimensional Plasmonic Nano-Antenna-Dots Array. *Anal. Chem.* **2012**, *84*, 4489−95.
(41) Banerjee, I.; Pangule, R. C.; Kane, R. S. Antifouling Coatings: Recent Developments in the Design of Surfaces That Prevent Fouling by Proteins, Bacteria, and Marine Organisms. *Adv. Mater.* **2011**, *23*, 690−718.



DOI: 10.1021/acssensors.8b01033
*ACS Sens.* XXXX, XXX, XXX−XXX